

Graph Attention Networks with LSTM-based Path Reweighting

Jianpeng Chen*

University of Electronic Science and
Technology of China
cjpcool@outlook.com

Yujing Wang*

Key Laboratory of Machine Perception, MOE,
School of EECS, Peking University
yujwang@pku.edu.cn

Ming Zeng*

Carnegie Mellon University
ming.zeng@sv.cmu.edu

Zongyi Xiang

University of Electronic Science and
Technology of China
xzongyi@foxmail.com

Yazhou Ren[†]

University of Electronic Science and
Technology of China
yazhou.ren@uestc.edu.cn

Abstract

Graph Neural Networks (GNNs) have been extensively used for mining graph-structured data with impressive performance. However, traditional GNNs suffer from over-smoothing, non-robustness and over-fitting problems. To solve these weaknesses, we design a novel GNN solution, namely Graph Attention Network with LSTM-based Path Reweighting (PR-GAT). PR-GAT can automatically aggregate multi-hop information, highlight important paths and filter out noises. In addition, we utilize random path sampling in PR-GAT for data augmentation. The augmented data is used for predicting the distribution of corresponding labels. Finally, we demonstrate that PR-GAT can mitigate the issues of over-smoothing, non-robustness and overfitting. We achieve state-of-the-art accuracy on 5 out of 7 datasets and competitive accuracy for other 2 datasets. The average accuracy of 7 datasets have been improved by 0.5% than the best SOTA from literature.

1 Introduction

Graph-structured data has emerged with many attentions recently since it reflects real-world data such as biological networks, social networks, citation networks, and Word Wide Web. Mining the graph structure is useful in various real-world problems. There have been many works focusing on semi-supervised learning on graph data [1, 2, 3, 4, 5], which model the non-euclidean space and learn the structural information in graph. Among them, the most notable branches of works are Graph Neural Networks (GNNs), which embed graph-structured data through feature propagation [6, 3, 7, 8, 9].

However, traditional GNNs have some potential problems. Firstly, most GNNs face the over-smoothing problem [10, 11, 12]. These works state that GNNs can be regarded as a message-passing method [13] with a low-passing filter. This results in exponentially information lost with the increment

*Equal contribution.

[†]Corresponding author.

of propagation steps. Many works concentrate on how to address the over-smoothing problem for deep GNNs [9, 14, 15]. Unfortunately, although current GNN SOTAs, such as GRAND [16], GraphMix [17] and S²GNN [15], have considered multi-hop information, they ignore the importance of different paths with various hops. Secondly, these GNNs lack robustness to graph attack [18, 19] because most GNNs cannot filter out the meaningless paths and noises. Essentially, the propagation step aggregates all neighborhoods’ information with noises, where some noisy nodes and edges may dominate during representation learning. In addition, the overfitting problem also exists in GNNs, especially for small datasets. To solve this problem, most methods focus on how to utilize unlabeled data for training. One direction is to use triplet loss [20, 21] for increasing the distance of nodes from inter-class and decreasing the distance of nodes from the intra-class. The other direction is to use data-augmentation techniques [22, 23] to regularize the training process. In this paper, we combine the two techniques.

To address issues above-mentioned, we propose Graph Attention Networks with LSTM-based Path Reweighting (PR-GAT). PR-GAT incorporates a LSTM-based path reweighting module into the graph attention network to differentiate the importance of different paths. Thus, PR-GAT can automatically filter out noises and encode the most useful path structural information for a specific task. In addition, triplet loss is leveraged in PR-GAT to augment the discernment power of this model. Meanwhile, we utilize the random paths generated by the sampling-based method for data augmentation. Specifically, we leverage the augmented data to regularize the model by encouraging it to predict the same distribution of corresponding labels.

Finally, we empirically demonstrate that our method can effectively avoid the issues of over-smoothing and non-robustness, while mitigate the issue of overfitting. We also illustrate that the impressive power of PR-GAT is not sensitive to different embedding dimensions. Moreover, we show the novel components proposed in this paper brings significant improvement in ablation experiments.

Our contributions can be concluded as follows:

- We propose a novel LSTM-based path reweighting module and incorporate it with graph attention networks. With this design, our model can automatically filter out noises and encode the most useful path structural information for a specific task.
- We utilize unlabeled data to generate pseudo-labels, and apply triplet loss on these pseudo-labels to regularize the customized attention module. To the best of our knowledge, this is the first work to adopt triplet loss in GNNs.
- As demonstrated by comprehensive analysis, the proposed PR-GAT model effectively mitigate the issues of over-smoothing, non-robustness and overfitting.

2 Related Work

Graph Representation Learning Given a graph G , node representation aims to learn the low dimensional vector representation \bar{F} of each node with its auxiliary information i.e. feature vector F , and its semantic information of graph G . There have emerged many methods for node embedding in recent years especially those based on deep learning methods. These methods can mainly be divided into two categories according to the input data. The first is sampling-based which use random walk [2, 24, 25] or others sampling strategy to sample sub-graph as the input data [7, 26], the advantage is that they can learn the local information of a graph, and run the model in very large graphs; The second is inputting the whole graph [3, 8], and conducting graph neural network on the graph to learn the information of both node attributes and graph structure. [5] disentangle the single representation of node attributes and graph structure into two different representations respectively. Another noteworthy line focuses on how to utilize the unlabeled data, which we will introduce later.

Graph Neural Networks Graph neural networks (GNNs) [1, 6] learn the semantic information of a graph for downstream tasks. They learn the l^{th} layer representations for i^{th} node by aggregating its neighbors’ information. The core difference of GNNs is the aggregation or message passing [13] methods. For example, for aggregation information, GCN [3] use the graph convolution layer, in advancing, GAT [8] use graph attention layer. Formally, $H^{(l)} \in \mathbb{R}^{n \times k}$ denote n nodes’ k -dimension representation in l^{th} layer with $H^{(0)=F}$, and $W \in \mathbb{R}^{k \times k'}$ be the weights of l^{th} layer, where k' is the

dimension of $(l + 1)^{th}$ layer. Then we have: $H^{(l+1)} = \sigma(AGGREGATE(A, H^{(l)}W^{(l)}))$, where $AGGREGATE(\cdot)$ is the specific methods for aggregating the neighbors' information by adopting normalized adjacent matrix A , $\sigma(\cdot)$ is non-linear activation function such as *ReLU* function in GCN.

Semi-Supervised Learning on Graph One direction is to assign pseudo-labels to unlabeled data. Another direction is to design powerful regularization methods for regularizing graph neural network, these regularization methods can be conducted to enhance the GNNs' generalization ability.

On the one hand, for utilizing the unlabeled data, [27] first uses neural network to infer pseudo-labels of unlabeled data. [28, 29] use label propagation for pseudo-labels in the field of computer vision. [30, 31] perform the label propagation and pseudo-labels methods in the field of GNN. Similarly, inspired by the field of face recognition [20], we perform the triplet-loss with pseudo-labels in our work to regularize the LSTM model for path weight generating.

Another direction attracting lots of attention is that of consistency loss in GNNs [14, 16, 17, 32, 33, 34]. For example, VBAT [32] and GraphVAT [33] first adopt consistency loss in GNNs by virtual adversarial training, GrpahMix [17] first introduce mixup strategy [35] in GNNs by utilizing linear interpolation between two nodes for data augmentation, GRAND [16] has performed DropNode method (which same as DropEdge [14]) to perturb the graph structure for data augmentation. Differently, we perform the random walk method to sample various but the same distribution nodes to construct various attention matrices, and then utilize consistency regularization method to encourage the model to predict the same distribution of prediction.

3 The Proposed Method

3.1 Overview

In this section, we present a semi-supervised learning framework, named Graph Attention Networks with LSTM-based Path Reweighting (PR-GAT) for node classification. As illustrated in Figure 1, given an adjacency matrix A and a feature matrix F , there are three steps in PR-GAT. The first step is to compress the original features $F \in \mathbb{R}^{n \times d}$ to low dimensional features $\tilde{F} \in \mathbb{R}^{n \times d'}$. The second step is to generate node embeddings \bar{F} which have aggregated the subgraph information and multi-hop information. The third step is to feed the node embeddings \bar{F} into a classifier for prediction. The second step contains two modules, the multi-hop GNN module aggregates the

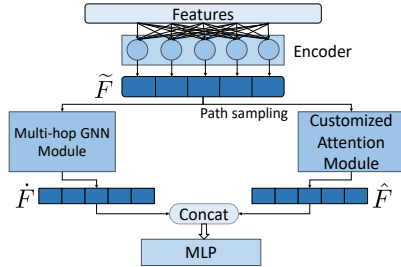


Figure 1: The architecture of PR-GAT.

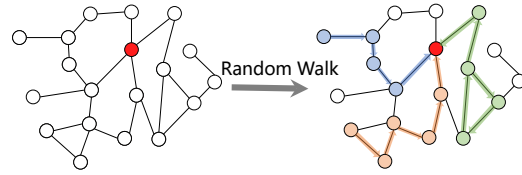


Figure 2: Sub-Graph Generation: colored paths make up a subgraph.

multi-hop information to \hat{F} , the customized attention module aggregates the subgraph information to \hat{F} . Finally, we concatenate \hat{F} and \hat{F} to get the expressive node embeddings \bar{F} . Next, we will introduce these modules and the training process in detail.

3.2 Feature Encoder

In the first step, a feature encoder f_{enc} is employed to compress the features $F \in \mathbb{R}^{n \times d}$ to low dimensional features $\{\tilde{F} \in \mathbb{R}^{n \times d'} | \tilde{F} = f_{enc}(F; \theta_1)\}$. The f_{enc} can be written as follow, $f_{enc}(F; W) = F \cdot W$, where $W \in \mathbb{R}^{d \times d'}$ is the trainable parameters represented as θ_1 in future.

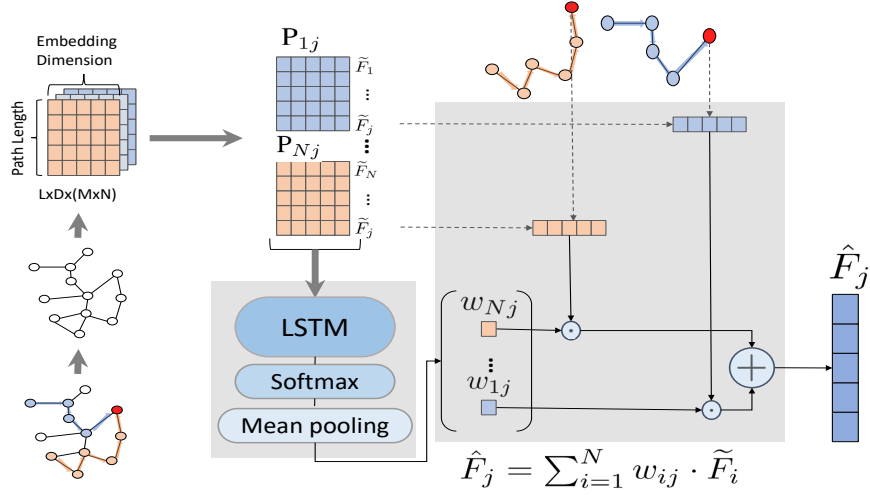


Figure 3: Detail of customized attention module.

3.3 Multi-hop GNN

Similar to other multi-hop GNN methods, we compute the means of all GNN layers' output. \dot{F} denotes the output of multi-hop GNN, the final value of \dot{F} is computed as follow:

$$\dot{F} = \frac{1}{H+1} \sum_{h=0}^H A^h \cdot \tilde{F}, \quad (1)$$

where H denotes highest order of this module.

3.4 Customized GAT (Graph Attention Networks)

Subgraph Generation Random walk could generate multiple paths P' and a number of node pairs. For example, setting the window size to 3 and path length to 4, we can get a path (n_1, n_2, n_3, n_4) and sub-paths from it, i.e. (n_1, n_2) , (n_2, n_1) , (n_2, n_3) , (n_3, n_2) , (n_3, n_4) , (n_4, n_3) , (n_1, n_2, n_3) , (n_2, n_3, n_4) , then, the weights between the start and end node in each sub-path are computed. To better understand the essence of these paths, as illustrated in Figure 2, the paths with the same endpoint can be seen as a subgraph, therefore, a subgraph is generated by multiple random walk processes, and we compute the weights (attentions) between each pair in the subgraph.

Path Re-weighting In the path re-weighting step, we generate path weight w_{ij} for node pair (x_i, x_j) , the critical point is how to extract the implicit information from paths P'_{ij} . On account of homophily assumption [36], the subgraph imply some semantic information about the labels, therefore, we can use natural language processing models like LSTM to catch the semantic information. *SIGMOID* activation function can compress the outputs of LSTM into range of $[0, 1]$, and then mean pooling is implemented for getting the path weight (attention) w_{ij} . Formally, we have node pair (x_i, x_j) and paths $P_{ij}^{(0)}, \dots, P_{ij}^{(k)}, \dots, P_{ij}^{(N-1)}$, the path weight w_{ij} can be computed by the followed formulation:

$$w_{ij} = \frac{1}{N} \sum_{k=0}^{N-1} \text{SIGMOID}(f_{lstm}(P_{ij}^{(k)}; \theta_2)), \quad (2)$$

where N , f_{lstm} and θ_2 denote the number of paths between node x_i and x_j , the LSTM model and the trainable parameters of LSTM respectively, path matrix $P_{ij} \in \mathbb{R}^{L \times D \times N}$ is the feature representation of path index P'_{ij} , where L , D and N represent the path length, dimension of \tilde{F} and the number of paths between node pair (x_i, x_j) .

Graph Attention These path weights $\{w_{ij}|0 \leq i, j < n\}$ are used to construct path attention matrix $W \in \mathbb{R}^{n \times n}$ whose role is similar to attention matrix in GAT or laplacian matrix in GCN.

For each path weight w_{ij} , there is a start point x_i and a end point x_j , for constructing the path attention matrix $\{W|W_{ij} = w_{ij}\}$, the index of start node i is treated as the row index of W , and the index of end node j is treated as the column index of W , naturally, we can get a sparse weight-matrix W each batch.

Graph Convolution In this step, we execute convolution operation on W to embed features \tilde{F} . This operation could aggregate the information of a subgraph to center node (j^{th} node) of this subgraph. The aggregate operation can be expressed as follow:

$$\hat{F}_j = \sum_{i=0}^{n-1} w_{ij} \cdot \tilde{F}_{ij}, \quad (3)$$

where w_{ij} is the attention (weight) value of i^{th} node to j^{th} node, n represents the number of nodes, and \hat{F}_j denotes the node embedding of j^{th} node.

Let D , L , M , and N denote the dimension of node embedding \tilde{F} , path length, number of center node, and path number of each center node. As illustrated in Figure 3, in the step of subgraph generation, $N * M$ paths P in dimension $L * D$ are generated, they are fed into the path re-weighting sub-module Section 3.4 for generating the path weights w_{ij} . Each path weight w_{ij} is an element of the path attention matrix W . Finally, the convolution equation can be written as follow:

$$\begin{aligned} W &= f_{pw}(P; \theta_2), \\ \hat{F} &= W \cdot \tilde{F}, \end{aligned} \quad (4)$$

where \hat{F} , \tilde{F} and W denote the matrix of aggregated node embeddings, encoded features and path attention matrix respectively, and $f_{pw}(P; \theta_2)$ is the path re-weighting process we have introduced in Eq (2), the input data P denotes the path matrix, and θ_2 is the trainable parameters of LSTM.

3.5 Classifier

The multi-hop information and subgraph information are aggregated in \hat{F} and \hat{F} respectively. We concatenate the outputs of the two modules, $\bar{F} = \hat{F} \oplus \hat{F}$, notation \oplus means concatenate operation. Then, we feed the node embeddings \bar{F} into classifier to get the prediction $Z \in \mathbb{R}^{n \times C}$ where C denotes the number of classes.

In PR-GAT, the classifier is a two layer MLP (input \rightarrow hidden \rightarrow output), the formulation can be written as $\bar{F}^{(l+1)} = RELU(\bar{F} \cdot w^{(l)} + b^{(l)})$, and then, we adopt *SOFTMAX* for prediction $\{Z|Z = SOFTMAX(\bar{F}^{(output)})\}$, where $\bar{F}^{(l+1)}$ means the output of l^{th} layer, the w and b represent the *weight* and *bias* of each MLP layer, and *SOFTMAX* and *RELU* are action functions. We use $Z = f_{mlp}(\bar{F}; \theta_3)$ to simplify this formulation, where θ_3 is the trainable parameters of MLP (w and b).

3.6 Training and Prediction

In this section, we introduce our training method in detail. The whole training and predicting process is stated in Algorithm 1. Then, we also discuss the limitations of PR-GAT in this section.

Triplet Loss The main idea of triplet loss is to make the weights in each subgraph become distinctive, which means that in the path attention matrix W , the weight w_{ij} is big if nodes (x_i, x_j) from the same subgraph, and the weight w_{ij} is tiny if nodes (x_i, x_j) from different subgraph. Therefore, we can get a more distinctive node embeddings after the convolution operation (See Section 3.4).

$$I_{ij} = \begin{cases} 1, & Y_i = Y_j \\ 0, & Y_i \neq Y_j \end{cases} \quad (5)$$

In doing so, we use matrix $I \in \{0, 1\}^{n \times n}$ to denote the label is same or not. In Eq (5), $Y_i \in \{0, 1\}^{n \times C}$ denotes the one-hot label vector, C represents the number of classes. Notably, the labeled i^{th} node

$Y_i \in Y^L$ is from training set directly, the unlabeled j^{th} node $Y_j \in Y^U$ is "guessed" by our model, $\{Y_j = \operatorname{argmax}(Z) | Y_j \in Y^U\}$, where Z denotes the probabilities predicted by PR-GAT. Then, the positive node pairs $(\hat{F}_i^{pos}, \hat{F}_j^{pos})$ and negative node pairs $(\hat{F}_i^{neg}, \hat{F}_j^{neg})$ can be sampled from I . We want to minimize the L_2 norm distance between positive node pairs and maximize the distance between negative node pairs. The loss function is as follows:

$$\begin{aligned}\mathcal{L}_{pos} &= \left\| \hat{F}_i^{pos} - \hat{F}_j^{pos} \right\|_2, \\ \mathcal{L}_{neg} &= RELU(m - \left\| \hat{F}_i^{neg} - \hat{F}_j^{neg} \right\|_2), \\ \mathcal{L}_{tri} &= \mathcal{L}_{neg} + \mathcal{L}_{pos},\end{aligned}\tag{6}$$

where m is a hyperparameter that represents the margin between negative node pairs. Additionally, to augment the power of encoder, triplet loss is also employed in \tilde{F} .

Consistency Regularization To better make use of the randomness of the path sampling strategy, we employ the consistency regularization [22] for avoiding overfitting.

In doing so, we generate S times of path attention matrix, the S path attention matrices conducted by S times convolution operation Section 3.4, and get S different feature matrices $\{\hat{F}^{(s)} | 1 \leq s \leq S\}$. We concatenate $\hat{F}^{(s)}$ with multi-hop GNN module's output feature \dot{F} to get $\{\bar{F}^{(s)} | \bar{F}^{(s)} = \dot{F} \oplus \hat{F}^{(s)}, 1 \leq s \leq S\}$, the features $\bar{F}^{(s)}$ are fed into MLP module to get the predictions $\{Z^{(s)} | Z^{(s)} = f_{mlp}(\bar{F}^{(s)}), 1 \leq s \leq S\}$. The S predictions $\{Z^{(s)} | 1 \leq s \leq S\}$ are used for consistency regularization.

The purpose of this regularization is to minimize the squared L_2 distance between the predictions $Z^{(s)}$, for example, setting $S = 2$, we want to get $\min \|Z^{(1)} - Z^{(2)}\|_2^2$. First, we sharpen [22] the prediction Z , in doing so, we need to get the average prediction $\bar{Z} = \frac{1}{S} \sum_{s=1}^S Z^{(s)}$ and sharpening the average probability \bar{Z}_{ij} of i^{th} node in j^{th} class with temperature T , i.e. $\bar{Z}'_{ij} = \bar{Z}_{ij}^{\frac{1}{T}} / \sum_{c=0}^{C-1} \bar{Z}_{ic}^{\frac{1}{T}}$, where \bar{Z}'_{ij} is the sharpened average prediction. Then, we compute the L_2 norm distance between the sharpened average prediction and other S prediction. At last, the consistency loss can be written as Eq (7):

$$\mathcal{L}_{con} = \frac{1}{S} \sum_{s=1}^S \sum_{i=0}^{n-1} \left\| Z_i^{(s)} - \bar{Z}'_i \right\|_2^2.\tag{7}$$

Unsupervised Loss Therefore, the unsupervised loss is a combination of the triplet loss and consistency loss showed in Eq (8), and we use two hyper-parameters λ_1 and λ_2 to control the balance of the two parts:

$$\mathcal{L}_{unsup} = \lambda_1 \mathcal{L}_{con} + \lambda_2 \mathcal{L}_{tri}.\tag{8}$$

Supervised Loss With labeled data Y^L and the predictions $Z^{(s),L}$ from MLP, we compute the average entropy loss of $\{Z^{(s),L} | 1 \leq s \leq S\}$:

$$\mathcal{L}_{sup} = -\frac{1}{S} \sum_{s=1}^S [Y^L \log Z^{(s),L} + (1 - Y^L) \log (1 - Z^{(s),L})].\tag{9}$$

Prediction To avoid the path attention matrix W being too sparse, we compute this matrix S times ($S = 4$ in our setting) and add them together to get a dense path attention matrix $\{W | W = \sum_{s=1}^S W^{(s)}\}$. The final path attention matrix is used to compute \hat{F} as Eq (4). Meanwhile, \dot{F} is computed by multi-hop GNN module. At last, the concatenated embedding \bar{F} is fed into classifier MLP to get the final prediction Z as we illustrated in Section 3.5.

Limitations The multi-Hop GNN module learns the graph structure information from high order neighborhoods, and the customized attention module aggregate the subgraphs' information. Both of

the two modules are based on homophily assumption [36]. Therefore, PR-GAT extremely depends on graphs with homophily.

Algorithm 1: PR-GAT

Input:

Data: adjacency matrix A , feature matrix F , training labels Y^L ;

Hyperparameters: loss tradeoff parameter λ , learning rate η , GNN propagation step H , times for regularization in each epoch S ;

Models: encoder $f_{enc}(F; \theta_1)$, path weight model $f_{pw}(P; \theta_2)$, MLP model $f_{mlp}(\tilde{F}; \theta_3)$.

Output:

prediction Z .

```

1 while not convergence do
2   initialize  $W$  with 0;
3   for  $s = 1$  to  $S$  do
4     Encode input features as Section 3.2:  $\tilde{F}^{(s)} = f_{enc}(F^{(s)}; \theta_1)$ ;
5     Aggregate multi-hop information via Eq (1) in Section 3.3:  $\dot{F}^{(s)} = \frac{1}{H+1} \sum_{h=0}^H A^h \cdot \tilde{F}^{(s)}$ ;
6     Constructing Path Attention Matrix from sampled paths as Eq (2):  $W^{(s)} = f_{pw}(P^{(s)}; \theta_2)$ ;
7     Get the final Path Attention Matrix:  $W = W + W^{(s)}$ ;
8     Aggregate subgraph information via Eq (4):  $\hat{F}^{(s)} = W^{(s)} \cdot \tilde{F}^{(s)}$ ;
9     Concatenate the two embeddings:  $\bar{F}^{(s)} = \dot{F}^{(s)} \oplus \hat{F}^{(s)}$ ;
10    Predict class probabilities as Section 3.5:  $Z^{(s)} = SOFTMAX(f_{mlp}(\bar{F}^{(s)}; \theta_3))$ ;
11  end
12  Compute the consistency regularization loss  $\mathcal{L}_{con}$  via Eq (7) and the triplets loss via Eq (6);
13  Compute the final unsupervised loss  $\mathcal{L}_{unsup}$  via Eq (8);
14  Compute the supervised loss  $\mathcal{L}_{sup}$  via Eq (9);
15  Update the parameters  $\theta_1, \theta_2$  and  $\theta_3$  by gradients descending:  $\Theta = \Theta - \eta \nabla_{\Theta}(\mathcal{L}_{sup} + \lambda \mathcal{L}_{unsup})$ ;
16 end
17 Output prediction  $Z$  as described in Section 3.6:  $Z = SOFTMAX(f_{mlp}(\dot{F}^{(s)} \oplus \hat{F}^{(s)}))$ .
```

4 Experiments

4.1 Experimental Setup

Our experimental setup strictly follow the previous standard settings in [37].

Dataset Following the community convention, we use three benchmark graphs, i.e. cora, citeseer and pubmed with their standard public split in Planetoid [2], fixed 20 nodes per class for training and 1000 nodes for testing. We also did experiments on 4 publicly available large datasets, i.e. Cora Full, Coauthor CS, Amazon Photo and Amazon Computers with their same experimental settings in [37]. The details of all datasets are introduced in Appendix A.1.

Baseline We choose three different genres for node classification task as the baseline, which include graph convolution based, sampling based and regularization based methods. We also include some recently published SOTAs [5, 9, 15, 16, 38]. For graph convolution based methods, we choose 12 significant methods; For sampling based methods, 2 methods i.e. GraphSAGE [7], FastGCN[39] are chosen to compare; For regularization based methods, we report 5 baselines with GCN as the backbone model and GRAND [16] with MLP as backbone model.

4.2 Results

Table 1 compares the accuracy of our model with 4 state-of-the-art methods, i.e. GCN [3], GAT [8], GRAND [16] and P-reg [30] on 7 node classification datasets. The results of all methods are reported in Appendix A.3. Our results successfully show that PR-GAT achieves state-of-the-art accuracy on 5 out of 7 datasets and competitive accuracy for other 2 datasets.

Table 1: Results on 3 standard split datasets and 4 large datasets with over 100 runs on different random seed for train/test set split and different random seed for weight initialization. **Bold** denotes the best performance, underline denotes the second best, and "-" denotes we do not run the experiment.

method	Cora	Citeseer	PubMed	Cora Full	Coauthor CS	Amazon Computers	Amazon Photo
GCN '2017	81.5	70.3	79.0	9.0±4.9	88.1±2.7	42.3±16.0	61.4±12.3
GAT '2018	83.0±0.7	72.5±0.7	79.0±0.3	13.7±5.2	90.3±1.4	65.4±15.3	80.8±9.5
GRAND '2020	85.4±0.4	75.4±0.4	82.7±0.6	<u>42.3±6.5</u>	92.9±0.5	80.1±7.2	72.9±2.1
P-reg '2020	82.8±1.2	71.6±2.2	77.4±1.5	—	92.6±0.3	81.7±1.4	91.2±0.8
PR-GAT(ours)	<u>85.3±0.6</u>	76.2±0.4	<u>82.1±0.3</u>	44.2±1.2	93.4±0.3	81.9±0.8	92.0±3.4

Table 2: Ablation study, the accuracy of PR-GAT without the specified component. The number in the parentheses is the decay of accuracy after remove this component.

Component	w\o multi-hop gnn	w\o customized attention	w\o triplet	w\o consistency	original
Cora	83.4(-0.9)	83.2(-2.1)	84.6(-0.9)	84.2(-1.1)	85.3
Citeseer	75.4(-0.8)	74.9(-1.3)	75.2(-1.0)	75.3(-0.9)	76.2
Pubmed	81.6(-0.5)	81.1(-1.0)	81.6(-0.5)	79.2(-2.9)	82.1

4.3 Ablation Study

Table 2 illustrate the results of an ablation study. This study evaluates the contributions of the different components in PR-GAT.

Without Customized Attention We only use the multi-hop GCN module, do not concatenate the embedding generated by path weight module \hat{F} , i.e. $\bar{F} = \hat{F}$.

Without Multi-hop GNN We only use the path weight module to generating the final node embedding, i.e. $\bar{F} = \hat{F}$. Then, in order to get a dense path attention matrix W from customized attention module, we sample paths for all nodes, i.e. setting batch size of path sampling to (#nodes / S).

Without Triplet Loss The unsupervised loss only computed by consistency regularization, and we do not employ the triplet loss for any independent node embedding.

Without Consistency Loss The unsupervised loss only computed by triplet loss. First, we set the hyperparameter $S = 1$ because that we do not need compute the sharpened prediction for consistency regularization. Second, we sample paths for all nodes to get a non-sparse path attention matrix. Third, because that there is not consistency regularization, we decrease the dropout rate in adjacency matrix to train a more stable model.

4.4 Analysis

We analyze how the proposed methods influence the results. To achieve this, we study three metrics of performance, i.e., generalization, robustness, and over-smoothing. Additionally, we analyze the influence of different embedding dimensions in Appendix A.3.1. We visualize the node embeddings by t-SNE in Appendix A.3.3.

Generalization Analysis We examine the generalization of PR-GAT and how PR-GAT's components contribute to its generalization. To measure this, we compute the gap of cross-entropy losses between train set and validation set. The smaller gap illustrate the better generalization ability of model. Figure 4 reports the results of the models, and proved that the techniques of customized attention module and triplet loss in PR-GAT can prevent overfitting.

Over-smoothing Analysis Lots of GNN models suffer the over-smoothing questions, as reported in some previous works [10, 15, 40], with the increase of orders, the identification of nodes in different

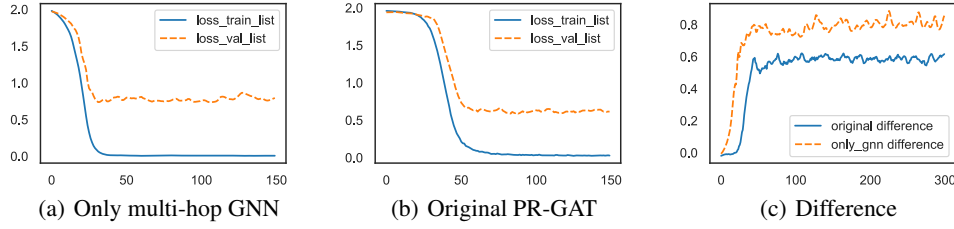


Figure 4: Losses on the original PR-GAT(b) and PR-GAT only multi-hop GNN(a), (c) is the variance between train loss and test loss of the two model. X axis denotes training epochs, Y axis denotes loss values.

classes become undistinguished, because that graph convolution aggregate the information from neighbor nodes, the multiple propagation step lead to over-mixing of information and noises [40], then, the node embeddings become similar. Figure 5 proved the ability of our models to relieve over-smoothing. It is obvious that the other GNNs, i.e. GAT and GCN are suffered from the over-smoothing problem, GRAND and PR-GAT has relieved the problem, and PR-GAT can always achieve the best results.

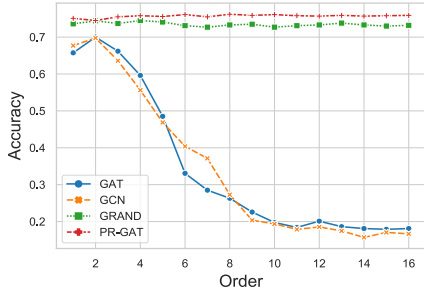


Figure 5: Over-smoothing analysis on Citeseer.

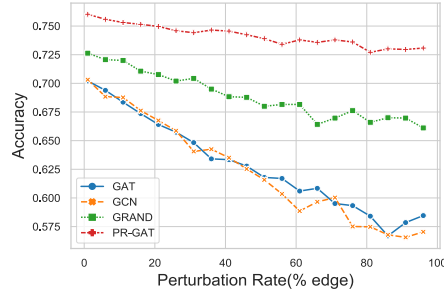


Figure 6: Robustness analysis on Citeseer.

Robustness Analysis We made a noise identification ability and robust analysis of PR-GAT by randomly adding a certain proportion of fake edges. Then, we observe the changes of the accuracy of node classification as the number of edges increases. In Figure 6, we gradually increase the perturbation rate (from 1% to 100%) and observe that the classification accuracy of nodes in GCN and GAT declines rapidly with the increase of fake edges. Although both PR-GAT and GRAND can maintain a slower decline rate in classification accuracy when the number of fake edges increases, we observe that the decline curve of PR-GAT is smoother than that of GRAND and consistently outperform GRAND at all perturbation rates on the Citeseer dataset.

5 Conclusions

In this work, we focus on the inherent issues existed in GNNs and present the Graph Attention Networks with LSTM-based Path Reweighting (PR-GAT). In PR-GAT, there contains two major modules. The first module is the multi-hop GNN that aggregates multi-hop information of graphs; The second module is the customized attention module. We utilize this module to aggregate the structural information of graphs and inject randomness to representation learning. Moreover, inspired by methods in computer vision, we perform triplet loss to better discern the node and utilize the randomness of the customized attention to regularize the model. Our experiments show that PR-GAT outperforms most SOTAs. We also empirically demonstrate the superiority of PR-GAT in terms of resistance to over-smoothing and the robustness to data attack. In future work, we aim to utilize the impressive expressive ability of PR-GAT and apply it to more graph-based tasks.

References

- [1] Marco Gori, Gabriele Monfardini, and Franco Scarselli. A new model for learning in graph domains. In *IJCNN*, 2005.
- [2] Zhilin Yang, William W. Cohen, and Ruslan Salakhutdinov. Revisiting semi-supervised learning with graph embeddings. In *ICML*, pages 40–48, 2016.
- [3] Thomas N. Kipf and Max Welling. Semi-supervised classification with graph convolutional networks. In *ICLR*, 2017.
- [4] Ming Ding, Jie Tang, and Jie Zhang. Semi-supervised learning on graphs with generative adversarial nets. In *CIKM*, pages 913–922, 2018.
- [5] Minghao Xu, Hang Wang, Bingbing Ni, Wenjun Zhang, and Jian Tang. Graphsadt: Learning graph representations with structure-attribute disentanglement. In *ICLR*, 2021.
- [6] Franco Scarselli, Marco Gori, Ah Chung Tsoi, Markus Hagenbuchner, and Gabriele Monfardini. The graph neural network model. *IEEE Transactions on Neural Networks*, 20(1):61–80, 2009.
- [7] William L. Hamilton, Zhitao Ying, and Jure Leskovec. Inductive representation learning on large graphs. In *NIPS*, pages 1024–1034, 2017.
- [8] Petar Veličković, Guillem Cucurull, Arantxa Casanova, Adriana Romero, Pietro Liò, and Yoshua Bengio. Graph attention networks. In *ICLR*, 2018.
- [9] Ming Chen, Zhewei Wei, Zengfeng Huang, Bolin Ding, and Yaliang Li. Simple and deep graph convolutional networks. In *ICML*, pages 1725–1735, 2020.
- [10] Qimai Li, Zhichao Han, and Xiao-Ming Wu. Deeper insights into graph convolutional networks for semi-supervised learning. In *AAAI*, pages 3538–3545, 2018.
- [11] Hoang NT and Takanori Maehara. Revisiting graph neural networks: All we have is low-pass filters. *CoRR*, abs/1905.09550, 2019.
- [12] Kenta Oono and Taiji Suzuki. Graph neural networks exponentially lose expressive power for node classification. In *ICLR*, 2020.
- [13] Justin Gilmer, Samuel S. Schoenholz, Patrick F. Riley, Oriol Vinyals, and George E. Dahl. Neural message passing for quantum chemistry. In *ICML*, pages 1263–1272, 2017.
- [14] Yu Rong, Wenbing Huang, Tingyang Xu, and Junzhou Huang. Dropedge: Towards deep graph convolutional networks on node classification. In *ICLR*, 2020.
- [15] Hao Zhu and Piotr Koniusz. Simple spectral graph convolution. In *ICLR*, 2021.
- [16] Wenzheng Feng, Jie Zhang, Yuxiao Dong, Yu Han, Huanbo Luan, Qian Xu, Qiang Yang, Evgeny Kharlamov, and Jie Tang. Graph random neural networks for semi-supervised learning on graphs. In *NeurIPS*, 2020.
- [17] Vikas Verma, Meng Qu, Alex Lamb, Yoshua Bengio, Juho Kannala, and Jian Tang. Graphmix: Improved training of gnns for semi-supervised learning. *CoRR*, abs/1909.11715, 2019.
- [18] Daniel Zügner, Amir Akbarnejad, and Stephan Günnemann. Adversarial attacks on neural networks for graph data. In *KDD*, page 2847–2856, 2018.
- [19] Dingyuan Zhu, Ziwei Zhang, Peng Cui, and Wenwu Zhu. Robust graph convolutional networks against adversarial attacks. In *KDD*, page 1399–1407, 2019.
- [20] Florian Schroff, Dmitry Kalenichenko, and James Philbin. Facenet: A unified embedding for face recognition and clustering. In *CVPR*, pages 815–823, 2015.
- [21] Xingping Dong and Jianbing Shen. Triplet loss in siamese network for object tracking. In *ECCV*, pages 472–488, 2018.
- [22] David Berthelot, Nicholas Carlini, Ian Goodfellow, Nicolas Papernot, Avital Oliver, and Colin Raffel. Mixmatch: A holistic approach to semi-supervised learning. In *NeurIPS*, pages 5050–5060, 2019.
- [23] Qizhe Xie, Zihang Dai, Eduard Hovy, Minh-Thang Luong, and Quoc V. Le. Unsupervised data augmentation for consistency training. In *NeurIPS*, 2020.
- [24] Bryan Perozzi, Rami Al-Rfou, and Steven Skiena. Deepwalk: Online learning of social representations. In *KDD*, pages 701–710, 2014.

- [25] Aditya Grover and Jure Leskovec. node2vec: Scalable feature learning for networks. In *KDD*, pages 855–864, 2016.
- [26] Wei-Lin Chiang, Xuanqing Liu, Si Si, Yang Li, Samy Bengio, and Cho-Jui Hsieh. Cluster-gcn: An efficient algorithm for training deep and large graph convolutional networks. In *KDD*, pages 257–266, 2019.
- [27] Dong-Hyun Lee. Pseudo-label: The simple and efficient semi-supervised learning method for deep neural networks. In *ICML*, 2013.
- [28] Ismail Elezi, Alessandro Torcinovich, Sebastiano Vascon, and Marcello Pelillo. Transductive label augmentation for improved deep network learning. In *ICPR*, pages 1432–1437, 2018.
- [29] Ahmet Iscen, Giorgos Tolias, Yannis Avrithis, and Ondrej Chum. Label propagation for deep semi-supervised learning. In *CVPR*, pages 5070–5079, 2019.
- [30] Han Yang, Kaili Ma, and James Cheng. Rethinking graph regularization for graph neural networks. *CoRR*, abs/2009.02027, 2020.
- [31] Zhongkai Hao, Chengqiang Lu, Zhenya Huang, Hao Wang, Zheyuan Hu, Qi Liu, Enhong Chen, and Cheekong Lee. Asgn: An active semi-supervised graph neural network for molecular property prediction. In *KDD*, pages 731–752, 2020.
- [32] Zhijie Deng, Yinpeng Dong, and Jun Zhu. Batch virtual adversarial training for graph convolutional networks. *CoRR*, abs/1902.09192, 2019.
- [33] Hongyang Gao and Shuiwang Ji. Graph u-nets. In *ICML*, pages 2083–2092, 2019.
- [34] Jiaqi Ma, Weijing Tang, Ji Zhu, and Qiaozhu Mei. A flexible generative framework for graph-based semi-supervised learning. In *NeurIPS*, pages 3276–3285, 2019.
- [35] Hongyi Zhang, Moustapha Cisse, Yann N. Dauphin, and David Lopez-Paz. mixup: Beyond empirical risk minimization. In *ICLR*, 2018.
- [36] Miller McPherson, Lynn Smith-Lovin, and James Matthew Cook. Birds of a feather: Homophily in social networks. *Annual Review of Sociology*, 27(1):415–444, 2001.
- [37] Oleksandr Shchur, Maximilian Mumme, Aleksandar Bojchevski, and Stephan Günnemann. Pitfalls of graph neural network evaluation. *CoRR*, abs/1811.05868, 2018.
- [38] Dongkwan Kim and Alice Oh. How to find your friendly neighborhood: Graph attention design with self-supervision. In *ICLR*, 2021.
- [39] Jie Chen, Tengfei Ma, and Cao Xiao. Fastgcn: Fast learning with graph convolutional networks via importance sampling. In *ICLR*, 2018.
- [40] Deli Chen, Yankai Lin, Wei Li, Peng Li, Jie Zhou, and Xu Sun. Measuring and relieving the over-smoothing problem for graph neural networks from the topological view. In *AAAI*, pages 3438–3445, 2020.
- [41] Diederik P. Kingma and Jimmy Lei Ba. Adam: A method for stochastic optimization. In *ICLR*, 2015.
- [42] Nitish Srivastava, Geoffrey Hinton, Alex Krizhevsky, Ilya Sutskever, and Ruslan Salakhutdinov. Dropout: a simple way to prevent neural networks from overfitting. In *JMLR*, pages 1929–1958, 2014.
- [43] Johannes Klicpera, Aleksandar Bojchevski, and Stephan Günnemann. Predict then propagate: Graph neural networks meet personalized pagerank. In *ICLR*, 2019.
- [44] Felix Wu, Amauri H. Souza Jr., Tianyi Zhang, Christopher Fifty, Tao Yu, and Kilian Q. Weinberger. Simplifying graph convolutional networks. In *ICML*, pages 6861–6871, 2019.
- [45] Meng Qu, Yoshua Bengio, and Jian Tang. GMNN: graph markov neural networks. In *ICML*, pages 5241–5250, 2019.
- [46] Yang Gao, Hong Yang, Peng Zhang, Chuan Zhou, and Yue Hu. Graphnas: Graph neural architecture search with reinforcement learning. *CoRR*, abs/1904.09981, 2019.

A Appendix

A.1 Datasets Details

These datasets can be downloaded from PyTorch-Geometric library¹. The datasets details are shown in Table 3.

Label rate is the fraction of nodes in training set (the number of training nodes are 20 per class) that can be computed as $(\text{\#class} \cdot 20) / \text{\#node}$. For large datasets, we remove the classes with too few nodes (2 classes with nodes less than 50) in Cora-Full for performing the split strategy. For standard planetoid datasets — Cora, Citeseer and PubMed — we use the default settings[2]. And the dataset split codes are included in our source code.

Table 3: Details of datasets after preprocessing.

Dataset	Nodes	Edges	Classes	Features	Label Rate
Cora	2708	5429	7	1433	0.0516
Citeseer	3327	4732	6	3703	0.0360
PubMed	19717	44338	3	500	0.0030
Cora-Full	19749	63262	68	8710	0.0689
Coauthor CS	18333	81894	15	6805	0.0164
Amazon Computer	13752	245861	10	767	0.0145
Amazon Photo	7650	119081	8	745	0.0209

A.2 Reproducibility

A.2.1 Implementation Details

We use PyTorch to implement PR-GAT and all of its components. The LSTM we used in customized attention module are implemented in package of torch.nn.LSTM. For Section 4, the results of GRAND are come from its public source code², the implementation of GCN and GAT layer from the PyTorch-Geometric library, and the results of P-reg taken from its original paper [30]. We adopt Adam[41] to optimize parameters of all models in our paper and we perform early stopping strategy to control the training epochs. We employ Dropout[42] in the adjacency matrix, path-weight matrix, encoder, and each layer of prediction module i.e. MLP, as a general used trick for preventing overfitting. The experiments of Cora, Citeseer are conducted on NVIDIA GeForce RTX 3070 Ti with 8GB memory size, the experiments of PubMed, Cora Full, Amazon Computer, Amazon Photo and Cauthor CS are conducted on Tesla V100 with 32GB memory size. As for software version, we use Python 3.8.5, Pytorch 1.7.1, NumPy 1.19.2, CUDA 11.0.

A.2.2 Hyperparameter Details

We show the hyperparameters of PR-GAT for results in Figure 5. These hyperparameters can be divided into 4 groups, the first control the training process which are shown in 1 to 12 rows of Table 4, the second controll the customized attention module which are shown in 13 to 16 rows of Table 4, the third control the triplet loss which are shown in 17 to 20 rows of Table 4, and the fourth control the the consistency loss which are shown in 21 to 22 rows of Table 4.

A.3 Additional Analysis

A.3.1 Dimensional Reduction Analysis

In reality, many nodes attach some auxiliary information, for example, each node on Cora-Full attaches a feature with 8710-dimension. Therefore, the high dimensional features expect low dimensional representations. In this experiment, we conduct encoder f_{enc} to reduce the feature dimension in the beginning, then, PR-GAT is compared with GRAND in different dimensions. As shown in

¹<https://pytorch-geometric.readthedocs.io>

²<https://github.com/Grand20/grand>

Table 4: Hyperparameters of PR-GAT for reproducing the results reported in Table 5.

Hyperparameters	Cora	Citeseer	PubMed
Learning rate η	0.01	0.01	0.1
Dropout rate of MLP layers	0.5	0.5	0.8
Dropout rate of encoder	0.6	0.6	0.5
Dropout rate of Path Weight Adjacency matrix	0.6	0.6	0.6
Dropout rate of Adjacency matrix	0.5	0.5	0.5
LSTM hidden units	128	128	128
Early stop epochs	300	200	100
L2 weight decay rate	5e-4	5e-4	5e-4
Triplet loss coefficient in Eq (8) λ_1	1.0	1.0	1.0
Consistency loss coefficient in Eq (8)	1.0	1.0	1.0
Tradeoff $\lambda \hat{F} \oplus \lambda \hat{F}$	1.0	10.0	1.0
Embedding dimension (output dimension of Encoder)	512	512	500
Batch size of path sampling	300	300	500
Path length of path sampling	10	10	6
Window size of path sampling	10	5	5
Orders/Layers of Multi-Hop GNN module	8	4	5
Number of negative sampling for triplet loss	5000	10000	5000
Number of positive sampling for triplet loss	15000	10000	5000
Margin of negative samples for triplet loss	0.1	1	1
Temperature of consistency loss T	0.5	0.5	0.2
Times for regularization S	4	4	4

Figure 7, with the decrease of dimension, the accuracy of GRAND declining, however, the accuracy of PR-GAT is stable. The result demonstrates that PR-GAT is not sensitive to different embedding dimensions.

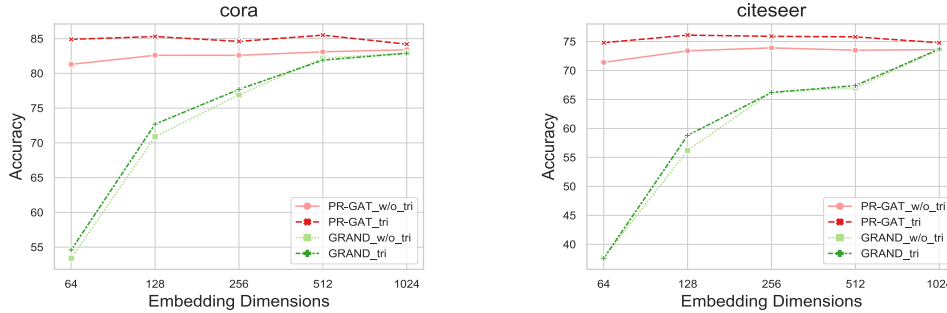


Figure 7: Analysis of dimension on Cora and Citeseer.

A.3.2 Over-Smoothing and Robustness Analysis on Cora

Figure 8 demonstrates that PR-GAT and GRAND both can effectively mitigate the issue of over-smoothing on Cora. In Figure 9, we can observe that the decay of PR-GAT is slowest, which demonstrates the strong power of PR-GAT in avoiding data attacking on Cora.

A.3.3 Visulization of the Learned Features

In order to study the features learned by PR-GAT on Citeseer dataset, we use the t-SNE to represent the 2-dimensional visualization of the hidden state (the output before the Classifier (MLP)). In Figure 10, we can see that features learned by PR-GAT are much better seperated than GCN and GAT obviously.

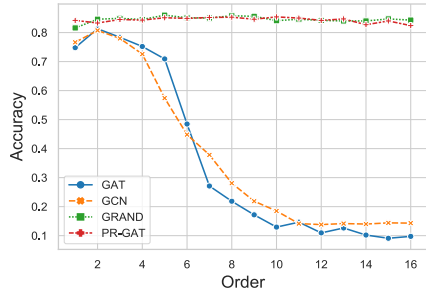


Figure 8: Over-smoothing analysis on Cora.

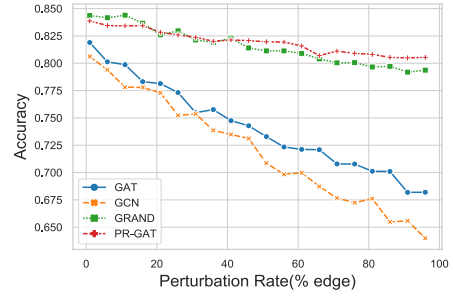


Figure 9: Robustness analysis on Cora.

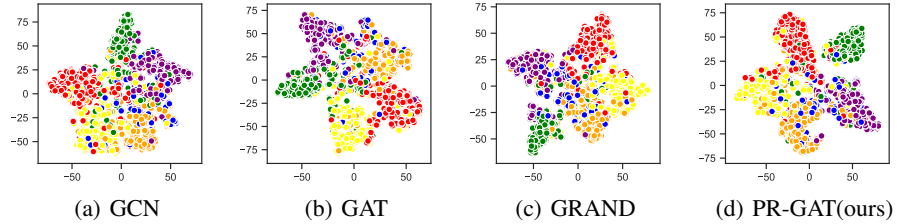


Figure 10: 2-dimensional representation of the hidden state of Citeseer dataset using (a)GCN, (b)GAT, (c)GRAND and (d)PR-GAT.

A.4 Additional Results

A.4.1 Comparison with State-of-the-art Methods

Table 5 reports the test accuracies of node classification on 3 datasets with public split. The results of baselines are taken from the original papers. The results of PR-GAT are averaged over 100 runs.

A.4.2 Results on Large Datasets

The experiments strictly follow the evaluation protocol used in [37]. Table 6 reports the accuracies of PR-GAT and 5 significant baselines on 4 large datasets. The results of two-layer MLP (input layer \rightarrow hidden layer \rightarrow output layer) with 128-hidden units, GCN, GAT, GRAND and PR-GAT are averaged over 100 runs on different random seed for train/test set split and different random seed for weight initialization. The results of P-reg are taken from its original paper [30]. The results show us that PR-GAT outperform the 5 significant baselines on the 4 large datasets.

Table 5: Overall results on three standard citation graph with standard split [2]. **Bold** denotes the best performance, underline denotes the second best and "*" denotes the third best.

method	Cora	Citeseer	PubMed
regularization			
VBAT (2019)[32]	83.6±0.5	74.0±0.6	79.9±0.4
G ³ NN (2019) [34]	82.5±0.2	74.4±0.3	77.9±0.4
GraphMix (2019)[17]	83.9±0.6	74.5±0.6*	81.0±0.6
DropEdge (2020)[14]	82.8	72.3	79.6
GRAND (2020)[16]	<u>85.4±0.4</u>	<u>75.4±0.4</u>	82.7±0.6
P-reg (2020)[30]	82.8±1.2	71.6±2.2	77.37±1.5
sampling based			
GraphSAGE (2017)[7]	78.9±0.8	67.4±0.7	77.8±0.6
FastGCN (2018)[39]	81.4±0.5	68.8±0.9	77.6±0.5
gnn based			
GCN (2017)[3]	81.5	70.3	79.0
GAT (2018)[8]	83.0±0.7	72.5±0.7	79.0±0.3
MixHop (2018)[35]	81.9±0.4	71.4±0.8	80.8±0.6
APPNP (2019)[43]	83.8±0.3	71.6±0.5	79.7±0.3
Graph U-Net (2019)[33]	84.4±0.6	73.2±0.5	79.6±0.2
SGC (2019)[44]	81.0±0.0	71.9±0.1	78.0±0.0
GMNN (2019)[45]	83.7	72.9	81.8*
GraphNAS (2019)[46]	84.2±1.0	73.1±0.9	79.6±0.4
GCNII (2020)[9]	85.5±0.5	73.4±0.6	80.2±0.4
superGAT (2021)[38]	84.3±0.6	72.6±0.8	81.7±0.5
S ² GC (2021)[15]	83.5±0.02	73.6±0.09	80.2±0.02
GraphSAD (2021)[5]	83±0.42	71.23±0.22	79.56±0.11
PR-GAT (ours)	85.3±0.6*	76.2±0.4	<u>82.1±0.3</u>

Table 6: Mean test accuracy and standard deviation on 4 large datasets with 100 runs each split strategy with 20 weight initialization strategy. **Bold** denotes the best performance, underline denotes the second best and "-" denotes we do not run this experiment.

method	Cora-Full	Coauthor CS	Amazon Computer	Amazon Photo
MLP	18.3±4.9	88.3±0.7	57.8±7.0	73.5±9.7
GCN (2017)[3]	9.0±4.9	88.1±2.7	42.3±16.0	61.4±12.3
GAT (2018)[8]	13.7±5.2	90.3±1.4	65.4±15.3	80.8±9.5
GRAND (2020)[16]	<u>42.3±6.5</u>	92.9±0.5	80.1±7.2	72.9±2.1
P-reg (2020)[30]	—	92.6±0.3	81.7±1.4	91.2±0.8
PR-GAT (ours)	44.2±1.2	93.4±0.3	81.9±0.8	92.0±3.4